Appl. Phys. B 78, 835–840 (2004)
DOI: 10.1007/s00340-004-1485-7

Applied Physics B
Lasers and Optics

R. LÓPEZ-MARTENS[1,✉]
J. MAURITSSON[1]
P. JOHNSSON[1]
K. VARJÚ[1,*]
A. L'HUILLIER[1]
W. KORNELIS[2]
J. BIEGERT[2]
U. KELLER[2]
M. GAARDE[3]
K. SCHAFER[3]

Characterization of high-order harmonic radiation on femtosecond and attosecond time scales

[1] Department of Physics, Lund Institute of Technology, P.O. Box 118, 22100 Lund, Sweden
[2] Department of Physics, Institute of Quantum Electronics, Swiss Federal Institute of Technology, Zürich, Switzerland
[3] Department of Physics and Astronomy, Louisiana State University, Baton Rouge, LA, USA

Received: 3 November 2003/Revised version: 15 January 2004
Published online: 22 April 2004 •

ABSTRACT We characterize the temporal structure of high-order harmonic radiation on both the femtosecond and attosecond time scales. The harmonic emission is characterized by mixed-color two-photon ionization with an infrared femtosecond laser using a Mach–Zehnder interferometer where both pump and probe arms travel completely separate paths. In a first experiment, we measure the duration and chirp of individual harmonics. In a second experiment, we resolve, for the first time with this type of setup, the attosecond beating of several harmonics generated under conditions similar to the first experiment. We suggest that the results of both measurements can be combined to determine the full attosecond time structure of the harmonic emission.

PACS 32.80.Rm; 42.65.Ky

1 Introduction

A unique property of the extreme ultraviolet (XUV) radiation obtained through high-order harmonic generation (HHG) is its ultrashort pulse duration [1–4]. This underscores the necessity of extending the techniques already used in the visible range, both for manipulating and characterizing ultrashort laser pulses, to the XUV window of the electromagnetic spectrum. The practical application of HHG in metrology experiments of fast electronic processes requires reliable methods for precise reconstruction of the temporal harmonic field, on both the femtosecond [5, 6] and attosecond time scales [3, 7, 8].

The broad coherent spectrum contained in an ultrashort laser pulse implies that the evolution in time of its constituent frequencies (frequency chirp) must be determined in order to accurately reconstruct its temporal shape. FROG [9] and SPIDER [10] are examples of already established techniques that are successful in mapping out the time–frequency distribution of femtosecond pulses in the optical frequency domain. The best method currently available for characterizing ultrashort pulses in the XUV domain is two-photon ionization (TPI) using a known infrared (IR) reference pulse [11, 12]. It is particularly well suited for XUV pulses obtained through HHG since the same laser driving the generation process can be used for the nonlinear photoionization and is perfectly synchronized to the XUV emission. The method consists in analyzing the TPI signal due to absorption of the XUV radiation and the known IR reference pulse delayed in time. This allows one to track the temporal evolution of the different XUV frequencies with respect to the phase of the infrared laser field.

2 Time–frequency characterization of high-order harmonic emission

Performing TPI measurements on XUV radiation obtained through HHG presents additional challenges that are directly related to the nature of the generation process itself. The laser-driven electron recollision picture proposed by Schafer et al. [13] and Corkum [14] is capable of reproducing many aspects of HHG. According to this picture, harmonics are generated by a sequence of collisions between the atom and electron wave packets formed by tunnel ionization near the peaks of the driving laser electric field. Measured HHG spectra emerge through the time-integrated interference of all the single encounters within the incident laser pulse duration and propagation of the generated XUV radiation through the target gas. This underlines the shortcomings of TPI in providing a full reconstruction of the temporal structure of HHG spectra: the amount of temporal information that can be recovered using this technique ultimately depends on the span of harmonic frequencies that can be sampled at the same time.

2.1 *Duration and chirp of individual harmonics*

If one samples the frequencies around each harmonic peak, by recording the TPI signal with a sufficiently short reference pulse one can successfully retrieve the temporal envelope and frequency chirp of singly isolated harmonic pulses [5]. The downside of this approach is twofold. First, in order to avoid having overlapping TPI signals from adjacent harmonics appearing in the photoelectron spectrum, it is desirable to use a reference pulse with a different frequency from

✉ Fax: +46-46/2224250, E-mail: rodrigo.lopez@fysik.lth.se
*On leave from the Department of Optics and Quantum Electronics, University of Szeged, Hungary

that of the driving laser field, thus imposing additional constraints on the already demanding experimental realization of such a technique [15, 16]. The other limiting aspect of this type of TPI measurement is the restricted spectral window of observation that allows the monitoring of only one harmonic pulse at a time, therefore making it impossible to retrieve any information concerning the interference in time between several harmonics.

2.2 *Attosecond beating of several harmonics*

Alternatively, if one expands the experimental window of observation to encompass several harmonics, one can trace the synchronization of emission of central harmonic frequencies within each half-cycle by recording the TPI signal with a reference pulse that is in phase with the driving laser field (i.e. a fraction of the driving laser field itself). The harmonic relationship between the frequency of the reference pulse and the harmonic frequencies (separated by twice the frequency of the reference pulse field) means that two consecutive harmonics can contribute to producing the same TPI signal. The observed oscillations in the TPI signal, as a function of delay (phase difference) of the reference pulse, reflect the difference in absolute phase of the two harmonics considered. By comparing the oscillations of the consecutive TPI signals in the total photoelectron spectrum, one can reconstruct the relative delay in emission of successive pairs of harmonics. In general, individual harmonics generated with pulses containing more than 10 cycles (FWHM) can be well resolved spectrally. Since the spectral amplitude drops quickly away from the central frequency, it is safe to concatenate the phase differences in order to get the relative phase difference between all the harmonics observed. Of course, the long duration of the reference pulse with respect to that of each individual harmonic pulses does not allow one to resolve the time-dependent frequency variation of the TPI signal, and thus the measurement only provides an average attosecond beating of the harmonic emission for all the oscillations of the driving laser.

2.3 *Experimental progress in Lund*

In this communication, we report the progress made in Lund in combining the measurement of individual harmonic duration and chirp together with that of attosecond beating between a bunch of harmonics in view of fully reconstructing the attosecond time structure of the harmonic spectrum. The advantage of the experimental setup is that the properties of the laser pulse driving the HHG process can be manipulated independently of those of the reference pulse. In a first experiment, we observe that it is possible to some extent to control the chirp of the individual harmonics generated in Argon by imposing a chirp on the driving laser pulse. We examine how the driving laser chirp is actually transferred to the different harmonics. In a second preliminary experiment, we could resolve the attosecond beating of several harmonics generated in Argon under conditions similar to the first experiment. This allows us to reconstruct the average shape of the attosecond pulse train generated around the peak of the driving laser pulse. Both measurements are complementary since a set of specifically synchronized harmonic wave packets with their individual amplitude and frequency chirp uniquely determines the temporal structure of the harmonic spectrum observed. It is easy to understand that within the field-driven recollision picture behind the HHG process, the attosecond time structure of the resulting harmonic emission will be directly affected by any change in oscillation frequency of the driving laser field. This offers promising prospects concerning the tailoring of the attosecond XUV emission.

3 Measuring the duration and chirp of harmonics 13 to 23 generated in Argon

3.1 *Narrowband TPI signal*

In this experiment (Fig. 1), we measure the duration and chirp of harmonics 13 to 23 generated in Argon using a variably chirped driving laser pulse (35 fs transform-limited duration). The TPI signal for these harmonics is obtained in Argon using a 12 fs reference pulse generated with a fraction of the same driving laser pulse [18].

As shown in Fig. 2, the TPI signal is made up of contributions from two neighboring harmonics and, unavoidably, the information extracted from the signal will be an average of the two contributing harmonics. Nevertheless, the duration and chirp of harmonics generated under these conditions are found to vary little between consecutive pairs of harmonics [15, 16], and one can decide to arbitrarily assign one TPI signal in the photoelectron spectrum to a particular neighboring harmonic peak. Under the present experimental conditions, the frequency- and delay-dependent intensity of the TPI

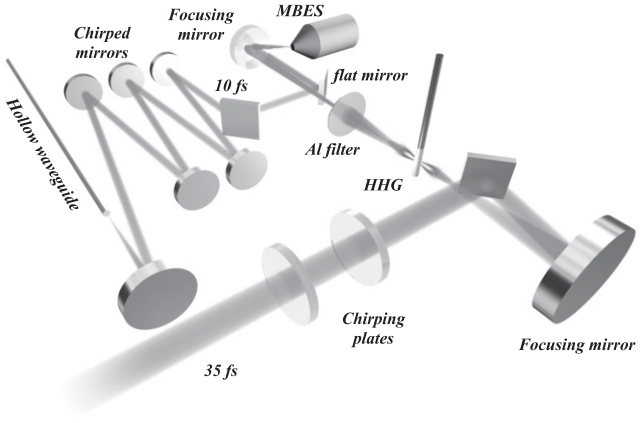

FIGURE 1 Experimental setup used to measure the duration and chirp of individual harmonics generated in Argon. The variably chirped infrared driving laser pulses (35 fs Fourier-transform limit at 815 nm) are focused into a 3 mm static Argon gas cell (30 mbar) with a 50 cm spherical mirror. The generated harmonics are filtered out from the remaining IR light and propagated in a vacuum to a magnetic bottle electron spectrometer (MBES) in which they are focused by a gold-coated spherical mirror with 20 cm focal length. A 12 fs reference pulse is generated through self-phase modulation of a fraction of the driving laser pulse in a gas-filled hollow-core fiber followed by recompression using chirped mirrors [18]. The reference pulse is then made to propagate parallel with the harmonic beam (flat mirror) and focused into the MBES at an angle of 2°. The TPI signal is recorded in the photoelectron spectrum of Argon as a function of delay between the harmonics and the reference pulse. The chirp rate of the driving pulse is varied by introducing material (chirping plates) in the driving beam and/or in the reference beam (prior to hollow fiber). By analyzing the driving and reference pulses online using SPIDER [19], we ensure that the reference pulse is always kept transform limited and that the driving pulse has the desired chirp

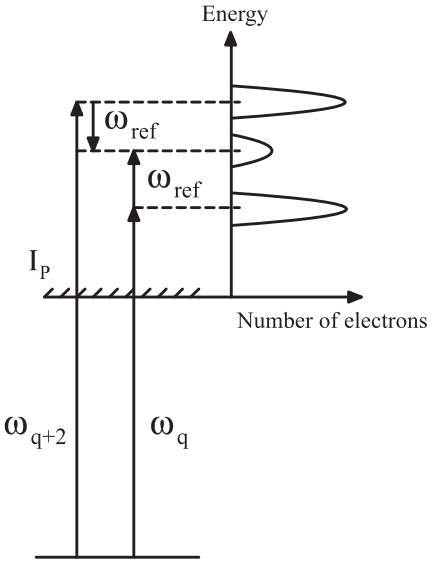

FIGURE 2 Origin of the TPI signal in the photoelectron spectrum: two consecutive harmonics ω_q and ω_{q+2} contribute to generating the TPI signal measured at ω_{q+1}

signal can be expressed as:

$$I_{\mathrm{TPI}}(\omega, \Delta t) \propto \left| \int_{\infty}^{\infty} \mathrm{d}t\, \mathrm{e}^{\mathrm{i}\omega t} \tilde{E}_{\mathrm{XUV}}(t) \tilde{E}_{\mathrm{ref}}(t - \Delta t) \right|^2, \qquad (1)$$

where ω is the energy of the TPI signal, Δt is the delay between the harmonics and the IR pulse, $\tilde{E}_{\mathrm{ref}}(t)$, the complex electric field amplitude of the reference pulse, and, $\tilde{E}_{\mathrm{XUV}}(t)$, the combined total complex electric field amplitude of the two adjacent harmonics.

Assuming both harmonics and IR pulses have Gaussian temporal shapes, the time duration of the harmonic can be extracted from the energy-integrated TPI signal (Fig. 3) by deconvolving it with the IR duration, τ_{IR}, according to

$$\tau_{\mathrm{XUV}} = \sqrt{\tau_{\mathrm{TPI}}^2 - \tau_{\mathrm{IR}}^2 - \tau_{\mathrm{geo}}^2}, \qquad (2)$$

where τ_{geo} is a geometrical factor accounting for the slightly noncollinear geometry of our experiment (estimated to be about 18 fs). Due to the finite duration of the reference pulse, the harmonic chirp has to be calculated from the observed frequency chirp, b_{TPI}, of the TPI signal (Fig. 3). The TPI signal is generated at the point of best temporal overlap between the two pulses, and the TPI energy measured at a certain time delay will therefore not correspond to the instantaneous energy of the harmonic pulse at that particular delay. The real chirp value for the harmonic is then given by

$$b_{\mathrm{XUV}} = b_{\mathrm{TPI}} \left[1 + \left(\frac{\tau_{\mathrm{IR}}^2 + \tau_{\mathrm{geo}}^2}{\tau_{\mathrm{XUV}}^2} \right) \right]. \qquad (3)$$

3.2 *Transfer of driving laser chirp to the harmonics*

Figure 4 presents the experimental TPI signal for harmonics 17 and 19 generated in Argon obtained for different chirp values imposed on the driving laser pulse while

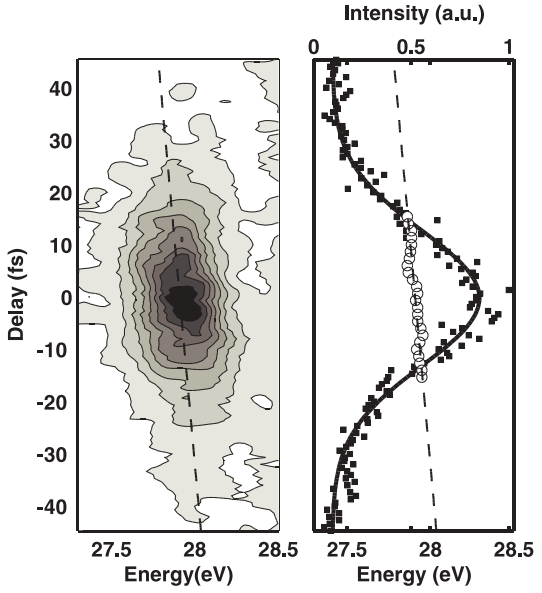

FIGURE 3 *Left:* Experimental TPI signal for harmonics 17 and 19 as a function of delay and energy. *Right:* energy-integrated TPI signal (*squares*) presented together with a Gaussian fit (*solid line*), and energy of the TPI signal maxima as a function of delay (*circles*) with a linear fit (*dashed line*)

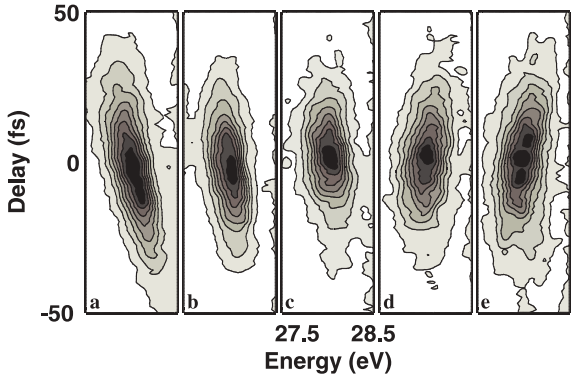

FIGURE 4 Experimental TPI signal for harmonics 17 and 19 as a function of delay and energy for different input chirps on the driving laser pulse (see Table 1)

maintaining a Fourier-transform limited reference pulse. An increase in chirp of the driving laser pulse necessarily stretches the pulse in time and leads to an undesired decrease of peak intensity. This can be partially compensated for by increasing the driving laser beam aperture prior to harmonic generation such that harmonics are generated with the same driving laser intensity. The compromise made here is that there might also be time-dependent changes in the phase-matching conditions contributing to the overall measured harmonic chirps shown in Table 1.

The transfer of driving chirp to the harmonics seems to be quite large, with harmonic chirp rates being at least one order of magnitude larger than those observed for Fourier-transform driving pulses. The degree of control that can be achieved on the individual harmonic chirp is beautifully illustrated by the way the chirp rates follow qualitatively the variation of the driving pulse chirp rate from negative to positive.

Figure 5 shows how the variation of chirp rate as a function of harmonic order depends on the chirp that is imposed

	a)	b)	c)	d)	e)	
I_{fund} (W cm^{-2})	1.0	1.8	1.5	1.9	1.6	$\times 10^{14}$
τ_{fund} (fs)	90	44	37	42	57	
τ_{XUV} (fs)	41	31	23	28	36	
b_{fund} (s^{-2})	−0.8	−1.1	0	0.89	1.2	$\times 10^{27}$
b_{XUV} (s^{-2})	−14	−11	−10	10	13	$\times 10^{27}$

TABLE 1 Driving laser pulse parameters (intensity, duration, and chirp rate) and extracted harmonic durations and chirp rates from the TPI signal corresponding to harmonics 17 and 19

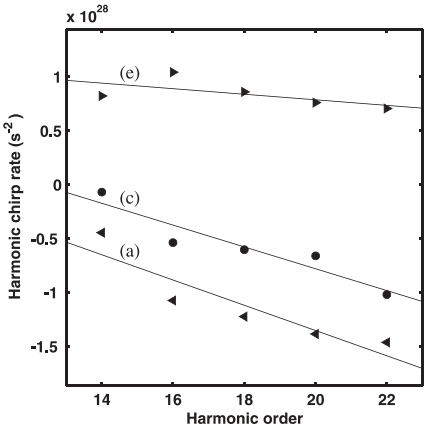

FIGURE 5 Measured harmonic chirp rates as a function of harmonic order for different input driving laser chirps (cases (a), (c), and (e) in Table 1)

on the driving laser. Harmonics generated with transform-limited or negatively chirped pulses exhibit a negative chirp rate decreasing with order, while adding a positive chirp on the driving pulse leads to harmonics with a positive chirp rate that is almost constant with order.

4 Recovery of an attosecond pulse train generated in Argon

4.1 *Broadband TPI signal*

The nature of the measurement is essentially the same as that of the method of RABBITT (reconstruction of attosecond beating by interference of two-photon transitions) proposed by Muller [17]. In this experiment (Fig. 6), we measure the beating on an attosecond time scale of harmonics 13 to 23 generated in Argon under conditions similar to those described in Sect. 3. Here, the harmonics are generated using transform-limited driving infrared pulses (35 fs at 800 nm), and the broadband TPI signal for all six harmonics is monitored using a fraction of the driving laser pulse itself as the reference pulse (35 fs). The collinear geometry of this experiment implies that we can now resolve the relative modulations of the individual TPI signal for each pair of harmonics on the time scale of the oscillations of the laser field.

As shown in Fig. 7, the broadband TPI signal appears at intermediate energies between adjacent harmonic energy peaks in the photoelectron spectrum, each separated by $2\omega_{\text{IR}}$, where ω_{IR} is the frequency of the infrared laser field. The origin of the interference in each individual TPI subpeak can be clearly seen if (1) is rewritten to explicitly show all phase terms con-

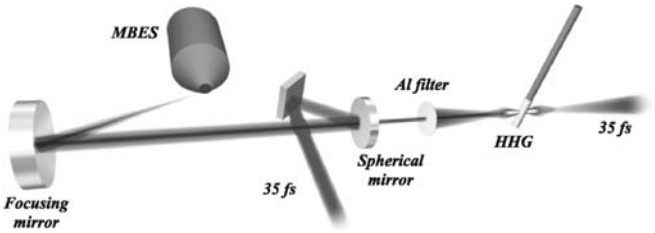

FIGURE 6 Experimental setup used to measure the attosecond beating of harmonics 13 to 23 generated in Argon under conditions similar to those described in Fig. 1. In this case, the driving laser pulses generating the harmonics are kept Fourier-transform limited (35 fs at 815 nm). The reference pulse is taken as a small fraction (equally transform limited) of the driving laser pulse itself (same frequency and phase). Prior to focusing into the electron spectrometer (MBES), the harmonics are passed through the hole in the middle of a spherical mirror placed under vacuum. This mirror is used to recombine both reference and harmonic beams and to make them propagate collinearly toward the MBES. The curvature of the spherical mirror is chosen such that the wavefront of the reference beam matches that of the harmonic beam at the point of focus inside the MBES. The TPI signal is then recorded in the photoelectron spectrum of Argon as a function of the phase difference between the harmonic and reference beams

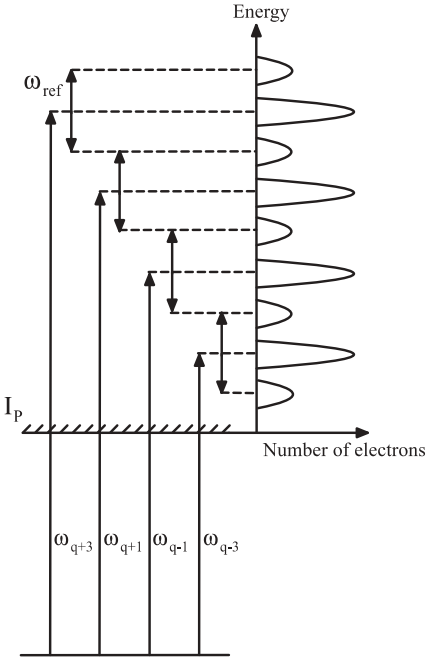

FIGURE 7 Origin of the broadband TPI signal in the photoelectron spectrum: consecutive pairs of harmonics contribute to generating a series of single TPI peaks spaced by twice the laser frequency ω_{IR}

tributing to the generation of the TPI signal, such that

$$I_{\text{TPI}}(\omega, \Delta t) \propto \left| \int_{\infty}^{\infty} \mathrm{d}t\, \mathrm{e}^{\mathrm{i}\omega t} |\tilde{E}_{\text{XUV}}(t)||\tilde{E}_{\text{IR}}(t-\Delta t)| \times \left[\mathrm{e}^{-\mathrm{i}\varphi_q}\mathrm{e}^{\mathrm{i}\omega_{\text{IR}}\Delta t} + \mathrm{e}^{-\mathrm{i}\varphi_{q+2}}\mathrm{e}^{-\mathrm{i}\omega_{\text{IR}}\Delta t}\right] \right|^2, \quad (4)$$

where $|\tilde{E}_{\text{XUV}}(t-\Delta t)|$ and $|\tilde{E}_{\text{IR}}(t-\Delta t)|$ are the envelopes of the XUV and infrared electric field amplitudes, φ_q and φ_{q+2} are the absolute phase of the adjacent harmonics that contribute to generating the TPI subpeak measured at $(q+1)\omega_{\text{IR}}$. The phase terms can be factorized, leading to an oscillatory term proportional to $\cos(2\omega_{\text{IR}}\Delta t + \Delta\varphi)$, where $\Delta\varphi = \varphi_{q+2} - \varphi_q$ is the relative phase difference between the

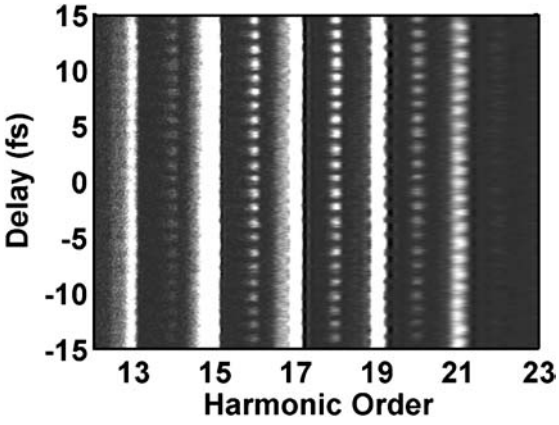

FIGURE 8 Experimental broadband TPI signal obtained for harmonics 13 to 23 as a function of delay and photoelectron energy

consecutive harmonic waves. This oscillatory behavior can be seen in the experimental TPI signal in Fig. 8, recorded for harmonics 13 to 23 generated in Argon. Each TPI subpeak varies between 0 and its maximum value with a periodicity of twice the reference laser frequency.

4.2 *Harmonic spectral phase*

The measured time shift between the individual TPI interference patterns allows one to extrapolate the relative phase difference between consecutive pairs of harmonics and, hence, to reconstruct the spectral phase of the sampled harmonics, albeit at intervals of $2\omega_{IR}$ [17]. This measurement will actually only give access to the relative variation, $\Delta(\Delta\varphi)$, of the phase difference between two consecutive harmonics from one pair of harmonics to another, which leads to an ambiguity in the absolute timing of emission of the harmonics with respect to the driving laser field. An absolute time reference with respect to the driving laser field is then required in order to lift this ambiguity [20, 21].

Figure 9 shows the different harmonic frequencies sampled in the broadband TPI measurement together with the reconstructed spectral phase (Yann Mairesse, private communication). The quadratic phase relationship observed between the sampled harmonics implies a constant delay in the time of emission (linear chirp) between consecutive harmonics estimated to be about 80 as, in good agreement with recent broadband TPI measurements performed in Argon [21]. As a consequence, the coherent superposition of all six harmonic frequencies will not lead to pulses with the shortest duration allowed by the their combined total bandwidth.

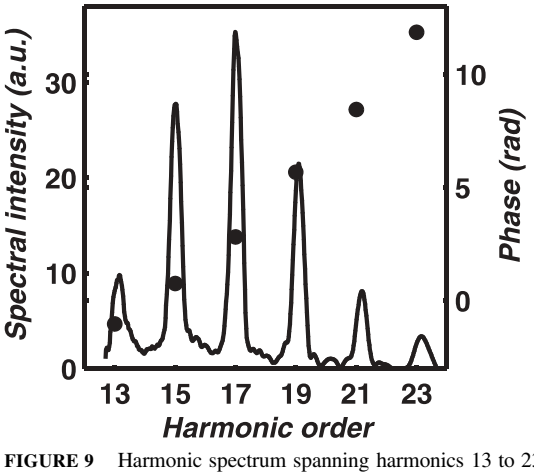

FIGURE 9 Harmonic spectrum spanning harmonics 13 to 23 generated in Argon and spectral phase (*circles*) reconstructed from the broadband TPI measurement

4.3 *Recovered attosecond pulse train*

The recovered shape of the attosecond pulse train resulting from the beating of these harmonics is presented in Fig. 10. The duration of each individual XUV burst in the train is calculated around 250 as, which is close to the Fourier limit of 202 as. The reconstructed pulse train shown here represents only an average of the attosecond time structure of the total harmonic field since there are many frequency components (with nonzero amplitude) around each central harmonic peak for which the spectral phase is not recovered by the broadband TPI measurement. The complete characterization of the attosecond time structure of the harmonic field would therefore require combining the results from both broadband and narrowband TPI measurements performed on harmonics generated under the exact same conditions. One way to accomplish this would be to use a short enough reference pulse to resolve the temporal structure of individual harmonics with a phase that can be controllably locked to that of the driving laser field. This puts severe (but not impossible) requirements on the stability of the experimental setup. Nevertheless, if these experimental requirements were to be fulfilled, the time-frequency distribution of all the individual TPI signals would contain sufficient information about the spectral phase to accurately reconstruct the electric field of the XUV radiation.

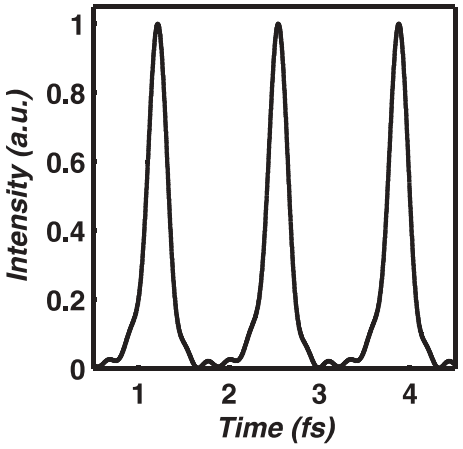

FIGURE 10 Temporal intensity profile of the attosecond pulse train recovered from the broadband TPI measurement. The duration of each individual XUV burst is approximately 250 as

5 Conclusion

In conclusion, we demonstrate the experimental implementation of two complementary TPI measurements in order to fully characterize high-order harmonic emission in

Argon using femtosecond pulses. We can control and characterize the duration and chirp of individual harmonic pulses and measure the synchronization of the central frequencies of different harmonic pulses without significantly changing the generation conditions. Combining the above measurements highlights the possibility of accurately controlling the attosecond temporal structure of harmonics in potential applications in time-resolved spectroscopy. To our knowledge, the observation of the attosecond time scale beating of harmonics using this type of Mach–Zehnder interferometer is the first of its kind.

ACKNOWLEDGEMENTS We acknowledge the support of the European Community's Human Potential Programme under contract HPRN-CT-2000-00133 (ATTO), the Knut and Alice Wallenberg Foundation, and the Swedish Science Council. K.S. acknowledges the support from the National Science Foundation through grant No. PHY-9733890. We also would like to thank Yann Mairesse for enlightening discussions during the HFSW meeting and for his valuable help in reconstructing the attosecond pulse train from our data.

REFERENCES

1 M. Ferray, A. L'Huillier, X.F. Li, L.A. Lompré, G. Mainfray, C. Manus: J. Phys. B **21**, L31 (1988)
2 L. Nugent-Glandorf, M. Scheer, D;A. Samuels, A.M. Mulhisen, E.R. Grant, X.M. Yang, V.M. Bierbaum, S.R. Leone: Phys. Rev. Lett. **87**, 193 002 (2001)
3 P.M. Paul, E.S. Toma, P. Breger, G. Mullot, F. Auge, P. Balcou, H.G. Muller, P. Agostini: Science **292**, 1689 (2001)
4 M. Drescher, M. Hentschel, R. Kienberger, M. Uiberacker, V. Yakovlev, A. Scrinizi, T. Westerwalbesloh, U. Kleineberg, U. Heinzmann, F. Krausz: Nature **419**, 803 (2002)
5 J. Norin, J. Mauritsson, A. Johansson, M.K. Raarup, S. Buil, A. Persson, O. Dühr, M.B. Gaarde, K.J. Schafer, U. Keller, C.G. Wahlstrom, A. L'Huillier: Phys. Rev. Lett. **88**, 193 901 (2002)
6 T. Sekikawa, T. Kanai, S. Watanabe: Phys. Rev. Lett. **91**, 103 902 (2003)
7 M. Hentschel, R. Kienberger, C. Spielmann, G.A. Reider, N. Milosevic, T. Brabec, P. Corkum, U. Heinzmann, M. Drescher, F. Krausz: Nature **414**, 509 (2001)
8 P. Tzallas, D. Charalambidis, N.A. Papadogiannis, K. Witte, G.D. Tsakiris: Nature **426**, 267 (2003)
9 R. Trebino, K.W. DeLong, D.N. Fittinghoff, J.N. Sweetser, M.A. Krumbugel, B.A. Richman, D.J. Kane: Rev. Sci. Instrum. **68**, 3277 (1997)
10 C. Iaconis, I.A. Walmsley: Opt. Lett. **23**, 792 (1998)
11 T.E. Glover, R.W. Schoenlein, A.H. Chin, C.V. Shank: Phys. Rev. Lett. **76**, 2468 (1996)
12 J.M. Schins, P. Breger, P. Agostini, R.C. Constantinescu, H.G. Muller, A. Bouhal, G. Grillon, A. Antonetti, A. Mysyrowicz: J. Opt. Soc. Am. B **13**, 197 (1997)
13 K.J. Schafer, B. Yang, L.F. DiMauro, K.C. Kulander: Phys. Rev. Lett. **70**, 1599 (1993)
14 P.B. Corkum: Phys. Rev. Lett. **71**, 1994 (1993)
15 R. López-Martens, J. Mauritsson, A. Johansson, J. Norin, A. L'Huillier: Eur. Phys. J. D **26**, 105 (2003)
16 J. Mauritsson, P. Johnsson, R. López-Martens, K. Varju, A. L'Huillier, W. Kornelis, J. Biegert, U. Keller: submitted to Phys. Rev. A
17 H.G. Muller: Appl. Phys. B **74**, S17 (2002)
18 M. Nisoli, S. DeSilvestri, O. Svelto, R. Szipöcs, R. Ferencz, C. Spielmann, S. Sartania, F. Krausz: Opt. Lett. **22**, 522 (1997)
19 W. Kornelis, J. Biegert, J.W.G. Tisch, M. Nisoli, G. Sansone, C. Vozzi, S. DeSilvestri, U. Keller: Opt. Lett. **28**, 281 (2003)
20 L.C. Dinu, H.G. Muller, S. Kazamias, G. Mullot, F. Augé, P. Balcou, P.M. Paul, M. Kovacev, P. Berger, P. Agostini: Phys. Rev. Lett. **91**, 063 901 (2003)
21 Y. Mairesse, A. de Bohan, L.J. Frasinski, H. Merdji, L.C. Dinu, P. Monchicourt, P. Berger, M. Kovacev, R. Taieb, H.G. Muller, P. Agostini, P. Salieres: Science **302**, 5650 (2003)